

Article

Performance of Fuzzy Inference System for Adaptive Resource Allocation in C-V2X Networks

Teguh Indra Bayu ^{1,2}, Yung-Fa Huang ^{3,*}  and Jeang-Kuo Chen ¹ ¹ Department of Information Management, Chaoyang University of Technology, Taichung 413310, Taiwan² Department of Informatics Engineering, Universitas Kristen Satya Wacana, Salatiga 50711, Indonesia³ Department of Information and Communication Engineering, Chaoyang University of Technology, Taichung 413310, Taiwan

* Correspondence: yfahuang@cyut.edu.tw

Abstract: Mode 4 of 3GPP Cellular Vehicle-to-Everything (C-V2X) uses a new Sensing-Based Semi-Persistent Scheduling (SB-SPS) algorithm to manage its radio resources. SB-SPS applies a probabilistic approach to provide the resource allocation in the system. The resource keep probability (P_{rk}) variable plays an essential role in the resource allocation mechanism. Most of the previous works used a fixed P_{rk} value. However, the Packet Delivery Ratio (PDR) can be improved by adapting the optimal P_{rk} value. Hence, we propose a Fuzzy Inference System (FIS) with two inputs, distance, and Channel State Information (CSI) to determine the suitable P_{rk} . The simulation results show that the proposed FIS method outperforms the other methods for sparse and congested road scenarios, with total numbers of vehicles at 200 and 400, respectively.

Keywords: C-V2X; mode 4; PDR; resource keep probability; CSI; Fuzzy Inference System



Citation: Bayu, T.I.; Huang, Y.-F.; Chen, J.-K. Performance of Fuzzy Inference System for Adaptive Resource Allocation in C-V2X Networks. *Electronics* **2022**, *11*, 4063. <https://doi.org/10.3390/electronics11234063>

Academic Editors: Jaime Lloret and Joel J. P. C. Rodrigues

Received: 31 October 2022

Accepted: 2 December 2022

Published: 6 December 2022

Publisher's Note: MDPI stays neutral with regard to jurisdictional claims in published maps and institutional affiliations.



Copyright: © 2022 by the authors. Licensee MDPI, Basel, Switzerland. This article is an open access article distributed under the terms and conditions of the Creative Commons Attribution (CC BY) license (<https://creativecommons.org/licenses/by/4.0/>).

1. Introduction

Advances in automotive network technology have encouraged the standardization of millimeter-wave wireless network technology [1]. The development of wireless technology, especially for vehicles, is divided into two standardizations, namely 802.11 or Wi-Fi technology and cellular network technology. One of the agencies regulating cellular network technology standardization is 3GPP, where 3GPP has formulated a Vehicle-to-Everything (V2X) standard that covers various kinds of vehicle communications, such as Vehicle-to-Vehicle (V2V), Vehicle-to-Infrastructure (V2I), Vehicle-to-Pedestrian (V2P), and Vehicle-to-Network (V2N) [2]. In terms of an autonomous vehicle (AV), a report [3] explained that integrating current LTE and 5G would unlock various advantages for electric cars and smart cars. The current computational resources could enable AV capabilities, and more technological challenges need to be assessed, from accident prevention to control systems. In the 3GPP release 14 standards, the Mode 4 communication type is defined as vehicle communication autonomously selecting and managing radio resources. To perform the task of autonomously managing resources, Mode 4 applies a new regulatory mechanism called Sensing-Based Semi-Persistent Scheduling (SB-SPS). The research in [4,5] describes the analytical model of SB-SPS Mode 4 in Long-Term Evolution (LTE) networks. A report [6] also discusses several parameters at the PHY and MAC layers that can affect the performance of Mode 4. The authors of [7] described the general range limits and blind spots that can occur in V2X communications.

Several previous studies have been conducted to further explore the potential and challenges in V2X technology, such as in [8], who tried to apply multiaccess technology to improve vehicle network performance. Research [9] applied Deep-Learning technology to perform resource management in Cellular V2X (C-V2X). Several other studies [10–12] also discussed resource management methods in V2X technology. A report [13] specifically proposed a solution to reduce the possibility of collisions in C-V2X broadcast communications.

Meanwhile, Ref. [14] discussed security countermeasures in C-V2X communication. Still related to the scheme of managing network resources in a vehicular network, Refs. [15,16] proposed a network slicing technique and path similarity selection to optimize the use of radio resources for future Fifth-Generation (5G) communications. In order to explore the potential of Mode 4 in particular, the authors in [17–19] proposed solutions of adaptive power management mechanisms and discussed the effects of using message delivery time intervals. A report [20] describes the performance of Mode 4 in congested highway conditions. The application of a Fuzzy Inference System (FIS) is also reported in [21], where dynamic resource management was carried out by applying Fuzzy Matching Learning. An integrated resource management mechanism was also reported in [22], prioritizing a Quality-of-Forwarding (QoF) mechanism in a C-V2X environment. A model of the LTE and 5G radio resource management mechanism using fuzzy detection is also reported in [23], which focuses on the optimal base station allocation mechanism.

Because radio resource availability is limited, SB-SPS applies a probability approach (P_{rk}) to enable the vehicle to autonomously reselect the radio resource slots. A report [24] explains that the P_{rk} probability approach can affect the performance of V2V and C-V2X Mode 4 communication. Authors [25] proposed an adaptive approach in using P_{rk} values with the help of CSI information as a consideration in making decisions. In [25], the decision-making method still uses an IF-statement logic approach. Authors [25] observed notable performance improvement by applying the matching table mechanism. However, the authors of [25] still employed a single variable for determining the final P_{rk} value, which is CSI. In this paper, we propose an FIS approach with multiple input variables to strengthen the dynamic P_{rk} value determination mechanism. Previous work was conducted in [26] to investigate the feasibility of FIS on V2V communications. In general, the main contributions of this work can be described as follows:

We conducted several simulations and found that the use of static P_{rk} values had not achieved optimal performance.

To explore the optimal solution to dynamically determine the P_{rk} value, we carried out an initial design approach using a matching IF-statement table. We used the vehicle distance and the Channel State Information (CSI) variable as a decision-making consideration.

The results of the initial design of the IF-statement matching table were then refined by applying FIS.

Performance measurement was carried out by comparing the PDR results for each scenario of fixed P_{rk} value, matching table, and FIS.

The remainder of the paper is structured as follows: Section 2 describes the technology. Section 3 describes the proposed FIS. Section 4 describes the simulation configuration and simulation results. Section 5 provides the conclusion of this work.

2. C-V2X Mode 4

2.1. Physical Layer

C-V2X employs Single-Carrier Frequency-Division Multiple Access (SC-FDMA) and can operate on 10 and 20 MHz channels. Each channel is broken down further into subchannels, as well as Resource Blocks (RBs), which are smaller subframes. Each subframe takes up one millisecond (like the Transmission Time Interval). The lowest possible amount of frequency resources that may be allotted to an LTE user is referred to as an RB. It has a frequency range that is 180 kHz broad (12 subcarriers of 15 kHz). A set of RBs that are contained inside the same subframe is what C-V2X refers to as a subchannel. The number of RBs that are allocated to each subchannel is variable. The transmission of data, as well as control information, makes use of subchannels. The information is sent across the wires using Transport Blocks (TBs). A Transmission Block (TB) stores the whole of a packet that is about to be broadcast, such as a beacon or a Cooperative Awareness Message (CAM)/Basic Safety Message (BSM). Transmission of TBs may be accomplished with either QPSK or 16-QAM with turbo coding. Each TB is sent out along with a Sidelink Control Information (SCI), which takes up two RBs in the same subframe and serves as a representation of

the signaling overhead for C-V2X Mode 4 communications. The SCI contains a variety of pieces of information, including the modulation and coding scheme that was used in the transmission of the TB, as well as the RBs that were utilized in the transmission of the TB. In order for other cars to be able to receive and interpret the sent TB signal, it is imperative that its reception be accurate. The highest power that may be transmitted is 23 dBm, and the specification states that the receiver's sensitivity power level must be -90.4 dBm [27].

2.2. Sensing-Based Semi-Persistent Scheduling

When operating in C-V2X Mode 4, cars make their own decisions on the resources they need without the aid of the cellular infrastructure. They make use of the sensing-based SPS scheduling method that was provided in Release 14 [28,29]. A vehicle holds the specified resource(s) for an undetermined amount of packets in a row before releasing them. This figure is dependent on either the time between packet transmissions or the number of packets that are transferred every second (λ). This random number is chosen between the ranges of 5 and 15, 10 and 30, and 25 and 75, when $\lambda = 10$ Hz, 20 Hz, and 50 Hz, respectively. When a vehicle needs to reserve additional resources, it picks a Reallocation Counter at random from its inventory. The Reallocation Counter is decreased by one after the completion of each transmission. When it reaches a value of zero, new resources have to be chosen and reserved with a chance of 1 over P_{rk} , with P_{rk} ranging from 0 to 0.8. In its SCI, each vehicle has both the value of its Reallocation Counter as well as the packet transmission interval that it uses. When making their reservation, vehicles make use of this information to estimate which resources are free so as to limit the likelihood of packet collisions. The act of reserving resources may be broken down into the following three stages for easier organization:

Step 1 is the stage for a vehicle (v_i) to reserve new resources inside an allocation window whenever it has to transmit a new packet, and the reallocation counter is at zero. The Allocation Frame is the temporal window that exists between the point in time at which the packet was created (t_b) and the maximum delay that was set. The highest delay for $\lambda = 10$ Hz is 100 milliseconds, for $\lambda = 20$ Hz is 50 milliseconds, and for $\lambda = 50$ Hz is 20 milliseconds [28]. The vehicle identifies the resources that it has the capacity to reserve while in the Allocation Frame. A resource is defined as a set of contiguous subchannels that are included inside the same subframe and provide sufficient space for the packet (SCI + TB) that is to be broadcast.

Step 2 is the stage for the vehicle (v_i) to construct a list of all the available resources (L_A) that it may reserve. All of the resources that were found in Step 1 are included in this list, with the exception of those that fulfill one of the two following requirements:

1. v_i has received an SCI from another vehicle during the last 1000 subframes, which indicates that it will use this resource in either the Allocation Frame or any of its subsequent Reallocation Counter packets. This information was obtained within the previous 1000 subframes.
2. v_i indicates whether or not the value of the Reference Signal Received Power (RSRP) of a resource is greater than a predetermined threshold.

Suppose vehicle (v_i) is transmitting during any prior subframe (f_j), where $j = i - 100 \cdot k$ and $k \in N, 1 \leq k \leq 10$ for $\lambda = 10$ Hz, then vehicle (v_i) excludes all of the resources of subframe (f_j) in the Allocation Frame. This occurs if vehicle (v_i) is operating at 10 Hz.

Following the completion of Step 2, L_A must include at least 20% of all the resources that were found in the Allocation Frame during Step 1. In the event that the 20% limit is not achieved, Step 2 is repeated until it reaches 20%. The RSRP threshold is raised by three decibels at the end of each repetition.

In Step 3, v_i compiles a list of candidate resources L_C , which contain those resources in L_A with the lowest average Received Signal Strength Indicator (RSSI). The size of the L_C has to be equivalent to twenty percent of all of the resources that were found in the Allocation Frame during Step 1. The value of RSSI is then averaged across all of the preceding $t_R - 100 \cdot j$ subframes ($j \in N, 1 \leq j \leq 10$) when λ is set to 10 Hz. After that,

vehicle v_t chooses one of the candidate resources in L_C at random, then set that resource aside for the subsequent Reallocation Counter broadcasts.

3. Proposed FIS

3.1. Matching Table Approach

In order to investigate the optimum solution, we first created a two-condition-based approach to leverage the possibility of P_{rk} value configurations. We call this approach a matching table condition. The first condition only required a single input variable, which was the vehicle distance to determine the final P_{rk} value on each data transmission. The second condition only required a single input variable, which was the CSI. The vehicle pairs were randomly selected on every transmission that occurs in the system. The matching table procedure can be explained as follows:

Step 1: Every vehicle distance is stored and recorded in the matrix v_{all} with the respective vehicle ID v_{ID} pairs.

Step 2: For every data transmission occurrence, the CSI matrix is recorded into the matrix v_{sense} .

Step 3: Use randomly selected v_{ID} pairs to extract the corresponding distance and CSI value for determining the P_{rk} value. We conducted two separate matching table scenarios, in which the first scenario only realized the distance value, and the second one realized the CSI value. The matching table based on the distance procedure can be explained by the following operations:

$$\begin{aligned} \text{If distance} \in [3, 30], \text{ then } P_{rk} &= 0.8. \\ \text{If distance} \in [30, 60], \text{ then } P_{rk} &= 0.7. \\ \text{If distance} \in [60, 90], \text{ then } P_{rk} &= 0.6. \\ \text{If distance} \in [90, 120], \text{ then } P_{rk} &= 0.5. \\ \text{If distance} \in [120, 150], \text{ then } P_{rk} &= 0.4. \end{aligned}$$

As distance is relatively short, the P_{rk} value was set to high. This means that the vehicles will tend to choose new resources for the following data transmissions. The matching table based on the CSI procedure can be explained by the following operations:

$$\begin{aligned} \text{If CSI} \in [0, 0.25], \text{ then } P_{rk} &= 0.2. \\ \text{If CSI} \in [0.25, 0.5], \text{ then } P_{rk} &= 0.4. \\ \text{If CSI} \in [0.5, 0.75], \text{ then } P_{rk} &= 0.6. \\ \text{If CSI} \in [0.75, 1], \text{ then } P_{rk} &= 0.8. \end{aligned}$$

Similar to the distance condition, while the network condition is sensed to have a low quality, the P_{rk} value is set to low. Hence, this condition makes the vehicles keep the current Resource Block for the following data transmissions. Figures 1 and 2 show the comparison between the two matching tables with a fixed P_{rk} value for $n_V = 200$ and 400 vehicles, respectively. It can be seen that the performance of the matching table approach is still lacking from the fixed P_{rk} value. A possible explanation for this might be that the final P_{rk} was only determined by a single variable. Even though the P_{rk} value was dynamically adapting to the given conditions, the current observations indicated unsatisfactory results.

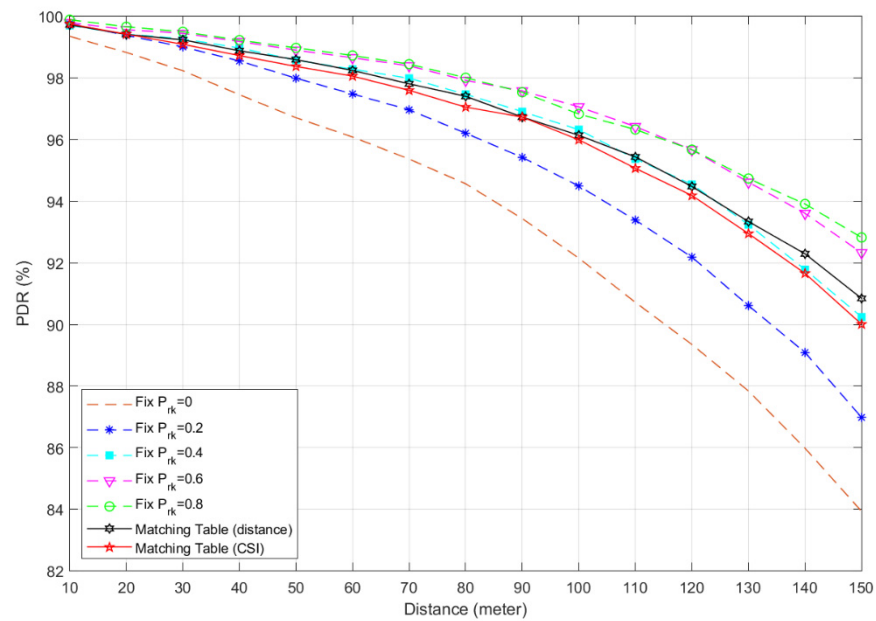


Figure 1. PDR performance comparison of matching table and fixed P_{rk} value for $n_V = 200$ -vehicle scenario.

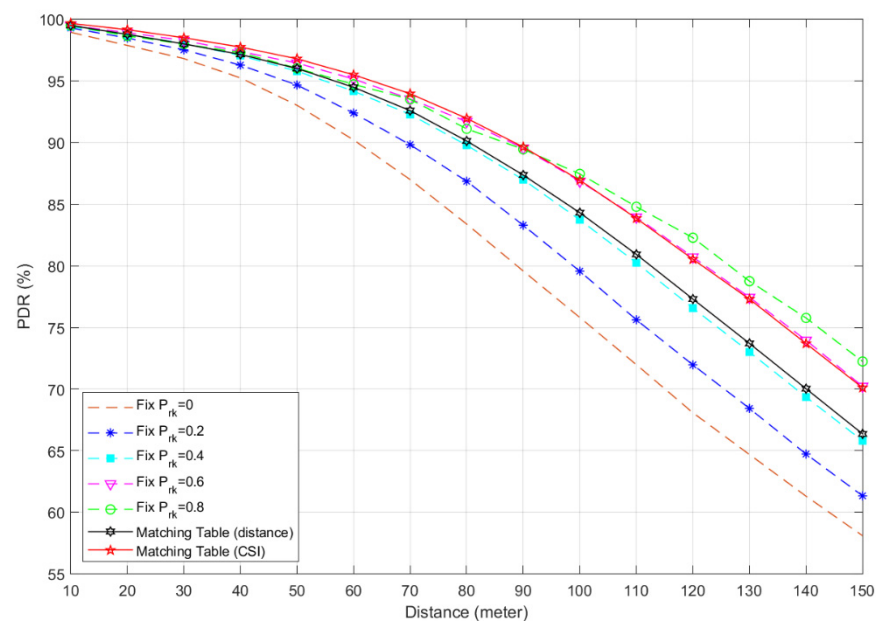


Figure 2. PDR performance comparison of matching table and fixed P_{rk} value for $n_V = 400$ -vehicle scenario.

3.2. Fuzzy Inference System Approach

To improve the performance of the matching table approach, we proposed an FIS for adaptive resource reallocation P_{rk} determination.

First, we designed and established fuzzy rule bases and membership functions (MBFs) for the input and output variables. We created the membership functions of P_{rk} according to the number of total vehicles, $n_V = 200$ and 400 vehicles, separately. Figure 3 shows the FIS, which consists of two inputs and one output. We designed a Mamdani fuzzy inference to construct a control system by integrating a set of linguistic form rules obtained from the matching table simulations. A total of 20 fuzzy rules were established to adjust P_{rk} as the fuzzy output variable. For the fuzzy input variable, the vehicle distance (d) was chosen as the first fuzzy input variable and the CSI as the second fuzzy input variable.

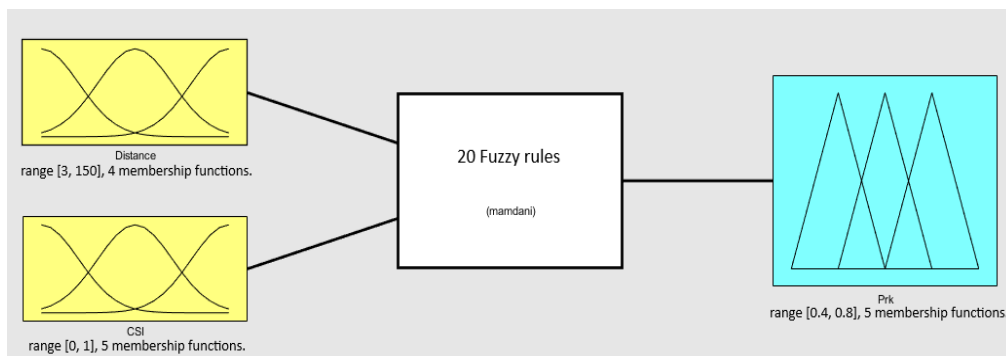


Figure 3. Proposed FIS structure.

The Gaussian combination membership function was chosen to cover the entire universe of discourse of the first input distance (d). The first fuzzy input range was set to [3 150] meters. Four linguistic terms: Short (Sh), Medium Short (MSh), Medium Far (MF), and Far (F), were chosen to cover the universe of discourse of distance (d), as shown in Figure 4. The mean value for the Short (Sh) was set to [−5 25]’ for Medium Short (MSh), to [45 65]; for Medium Far (MF), to [85 105]; and we set Far (F) to [125 155]. The given threshold value was chosen from the initial observations of the fixed P_{rk} simulations. We analyzed and designed the curve according to the highest PDR results from the fixed P_{rk} observations.

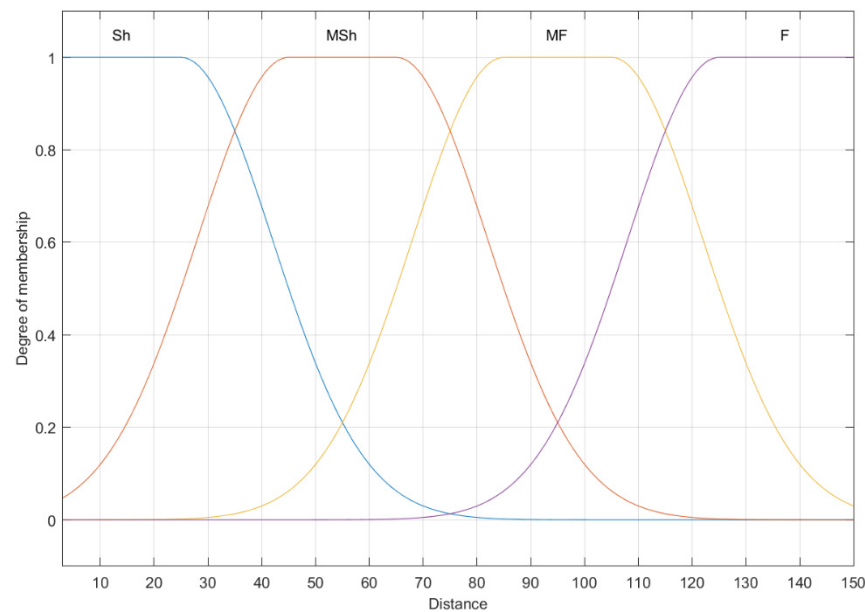


Figure 4. Fuzzy membership function for the first input distance (d).

The Gaussian membership function was chosen for the second fuzzy input and the fuzzy output, named CSI and P_{rk} , respectively. The ranges for CSI and P_{rk} were set to [0 1] and [0.4 0.8], respectively. The five linguistic terms chosen to represent the universe of discourse for the CSI were: Very Weak (VW), Weak (W), Average (Av), Strong (St), and Very Strong (VSt), as shown in Figure 5. The mean values for the second fuzzy input CSI were as follows: Very Weak (VW) was set to [0], Weak (W) to [0.25], Average (Av) to [0.5], Strong (St) to [0.75], and Very Strong (VSt) was set to [1]. Again, the curve was designed based on the initial fixed P_{rk} observations.

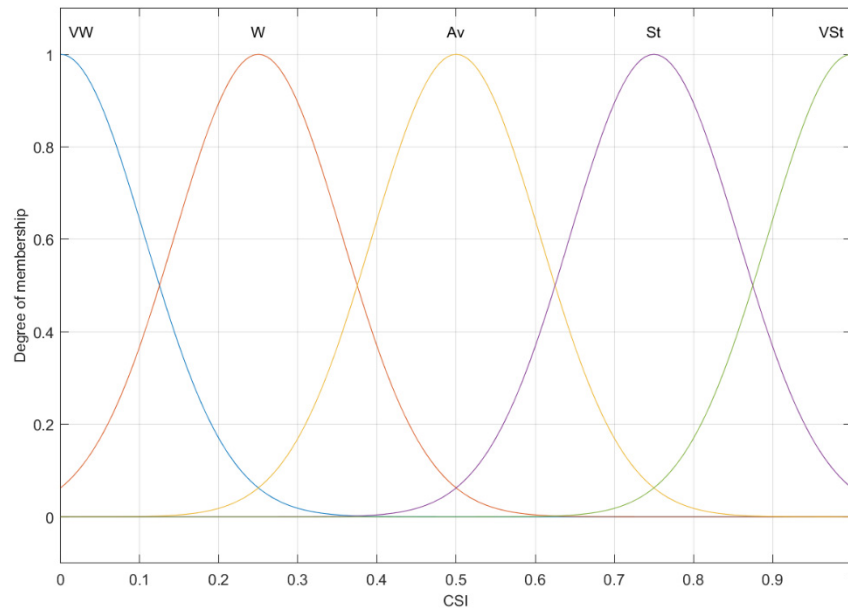


Figure 5. Fuzzy membership function for the second input CSI.

As for the fuzzy output, five linguistic terms were also chosen to explain the universe of discourse for P_{rk} : Very Low (VL), Low (L), Middle (Md), High (H), and Very High (VH), as shown in Figure 6. The fuzzy output range value [0.4 0.8] was chosen because the highest PDR performance from the initial observation only indicated the corresponding P_{rk} range. The mean values for the Very Low (VL), Low (L), Middle (Md), High (H), and Very High (VH) terms were set to: [0.4], [0.5], [0.6], [0.7] and [0.8], respectively.

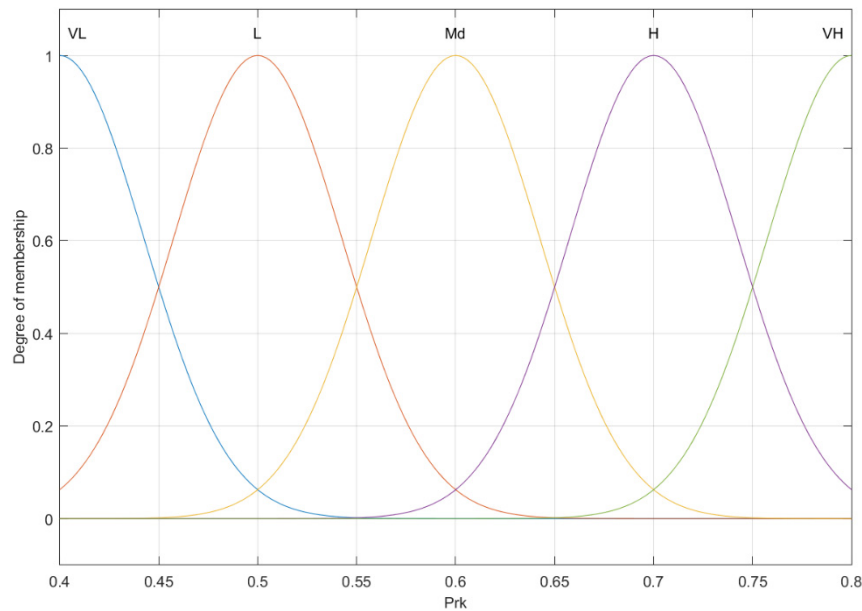


Figure 6. Fuzzy membership function for output P_{rk} .

The Gaussian membership function is usually represented as Gaussian($x:c,s$), where c and s represent the mean and standard deviation, respectively. The membership function of fuzzy set A , μ_A can be expressed by

$$\mu_A(x, c, s, m) = \exp\left[-\frac{1}{2}\left|\frac{x - c}{s}\right|^m\right] \tag{1}$$

where c represents the center, s represents the width, and m represents the fuzzification factor.

The fuzzy control rule follows IF-THEN rules with two inputs and one output and can be expressed by [30]

$$R_j : \text{IF distance}(d) \text{ is } F_1^{l_1} \text{ AND CSI is } F_2^{l_2} \text{ THEN } P_{rk} = F_3^{l_3} \tag{2}$$

where $F_1^{l_1}$, $F_2^{l_2}$, and $F_3^{l_3}$ are the linguistic terms that represent the two inputs' distance and CSI, and the output P_{rk} , respectively; l_1, l_2 , and l_3 are the index of the membership function for the input distance (d), CSI, and the output P_{rk} , respectively; $j = 1, 2, \dots, 20$ is the index of the fuzzy rule, as can be seen in Table 1. Figure 7 shows the overall 3D diagram for the proposed FIS.

Table 1. The rule bases for the proposed FIS.

Distance	Channel State Information	Resource Keep Probability
Sh	VW	VL
Sh	W	L
Sh	Av	Md
Sh	St	H
Sh	VSt	H
MSh	VW	L
MSh	W	Md
MSh	Av	H
MSh	St	H
MSh	Vst	Md
MF	VW	L
MF	W	L
MF	Av	Md
MF	St	Md
MF	VSt	Md
F	VW	Md
F	W	Md
F	Av	H
F	St	VH
F	VSt	VH

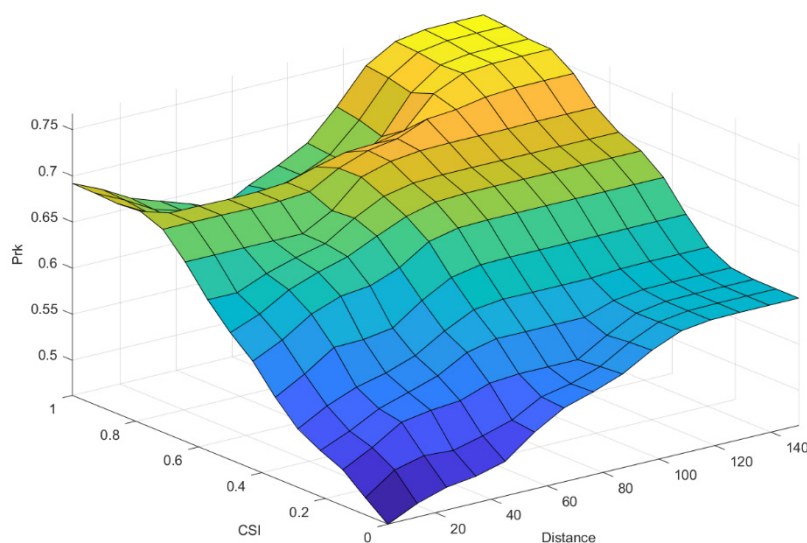


Figure 7. The relationships of inputs and output in the proposed FIS with a 3D diagram.

4. Simulation Results

We simulated a 2 km highway scenario with three lanes in each direction. The vehicle speed was set to 80 km/h with a 40 km/h standard deviation. The first scenario consisted of 200 vehicles in total (n_V), and the second scenario will consist of 400 vehicles. For each n_V , a simulation was run for the fixed P_{rk} scenario with $P_{rk} = 0, 0.2, 0.4, 0.6,$ and 0.8 ; the matching table for the distance and CSI scenarios; and the proposed FIS methods.

The PDR is the ratio of correctly delivered packets to the total number of transmitted packets. The PDR performance was plotted with the distance axes ranging from 0 to 150 m.

$$PDR = \frac{\text{Number of successfully delivered packets}}{\text{Total number of transmitted packets}} \tag{3}$$

The simulation was carried out based on the Monte Carlo method to investigate the effect of Resource Keep Probability on PDR performance. The random number seed we applied during the simulation was 1000, and each scenario was run 300 times.

Figure 8 shows the simulation results for the fixed P_{rk} values of 0, 0.2, 0.4, 0.6, and 0.8. We conducted various simulation configurations with the corresponding fixed P_{rk} values. The most interesting finding was that none of the fixed P_{rk} value configurations could achieve 99% PDR performance for the given distance range. For the condition $n_V = 200$, the P_{rk} values 0.6 and 0.8 were observed to produce almost similar results, while the $P_{rk} = 0$ configuration produced the poorest performance. Similar situations occurred for the $n_V = 400$ condition, where the P_{rk} values 0.6 and 0.8 presented similar results, and the worst performance occurred when $P_{rk} = 0$. These are particularly useful findings, that the P_{rk} value has an important effect on PDR performance. Furthermore, a single fixed P_{rk} value is not always superior to another fixed value. As can be seen in both n_V conditions, P_{rk} 0.6 and 0.8 seemed to overcome one another at a certain distance. For instance, in the $n_V = 200$ condition, the highest performance shifting occurred at distances of 90 m and 120 m. For $n_V = 400$, the highest performance shifting occurred at a distance of 90 m. The present simulations raise the possibility that an adaptive P_{rk} value assignment can improve PDR performance.

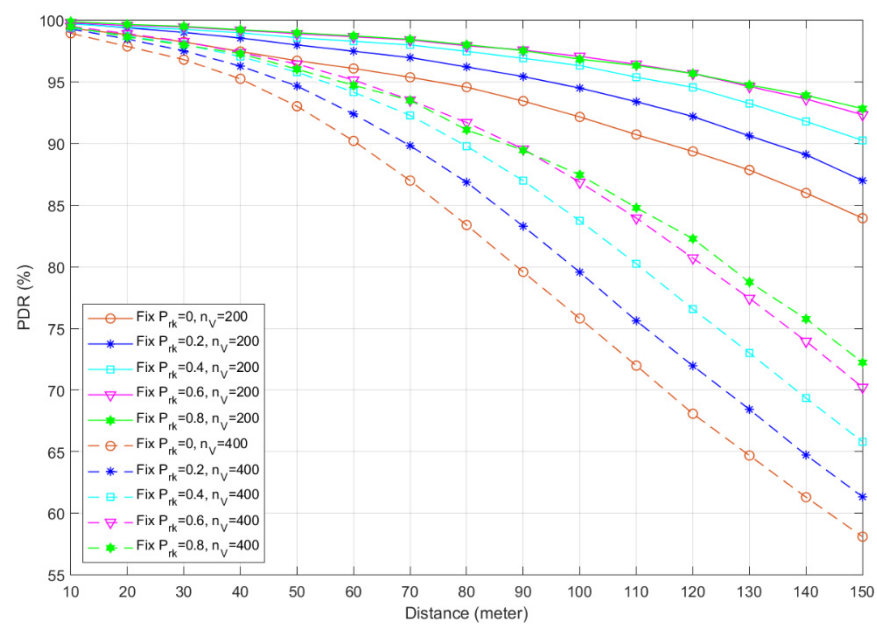


Figure 8. PDR performance of fixed P_{rk} values for total vehicle numbers of $n_V = 200$ and 400.

We used an LTEV2Vsim [31] simulator based on MATLAB, developed and shared by University of Bologna, National Research Council (CNR), and National Inter-University Consortium for Telecommunications (CNIT) - Italy. The detailed parameter settings are

shown in Table 2. The simulation time (T) was 60, with a position update time resolution (t_r) of 0.1 s. The channel models used in the simulation were Line of Sight (LOS) and Non-Line of Sight (NLOS) for various V2V communications.

Table 2. Parameter settings.

Parameter	Value
Simulation time	60 s
Vehicle position update time	0.1 s
Vehicle speed	80 km/h
Vehicle speed standard deviation	40 km/h
Road length	2000 m
Number of lanes	3 per directions
Total number of vehicles (n_V)	200, 400
Bandwidth	10 MHz
Transmission power	23 dBm
Beacon size	190 Bytes
Modulation coding scheme (MCS)	7
Sensing interval	0.1 s
Probability resource keep (P_{rk})	0, 0.2, 0.4, 0.6, 0.8
SINR threshold	8.47 dB

This section presents evaluation of the comparison of the fixed P_{rk} value simulation, the matching table, and the proposed FIS methods. Figures 9 and 10 show the corresponding $n_V = 200$ and $n_V = 400$ vehicles scenarios, respectively. At a glance, it can be observed that the overall performance of the $n_V = 400$ simulations produced lower results than the $n_V = 200$ simulations. This occurred because of the difference in the number of vehicles. More vehicles in the system mean more interference in the wireless network; in addition, more vehicles scramble for the radio resources. From Figures 9 and 10, we can observe that even though the SB-SPS uses a probability approach (P_{rk}) to manage the radio resource allocation, the fixed P_{rk} value cannot achieve the best performance. From the figures, the colored dash lines represent the fixed P_{rk} values of 0, 0.2, 0.4, 0.6, and 0.8. The black colored lines represent the two conditions from the matching table scenarios. The solid red line is the result of the proposed FIS method.

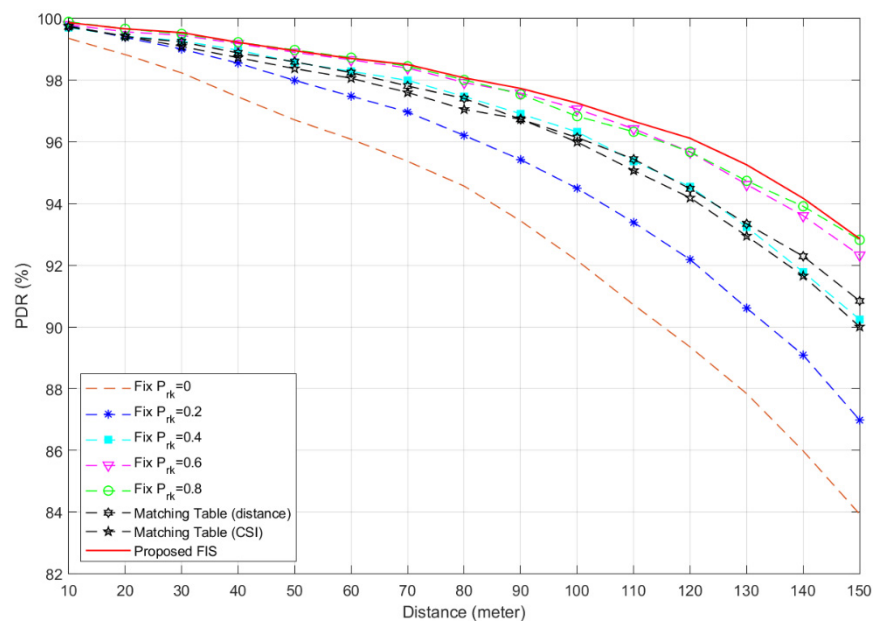


Figure 9. Overall PDR performance comparison for $n_V = 200$ vehicle scenario.

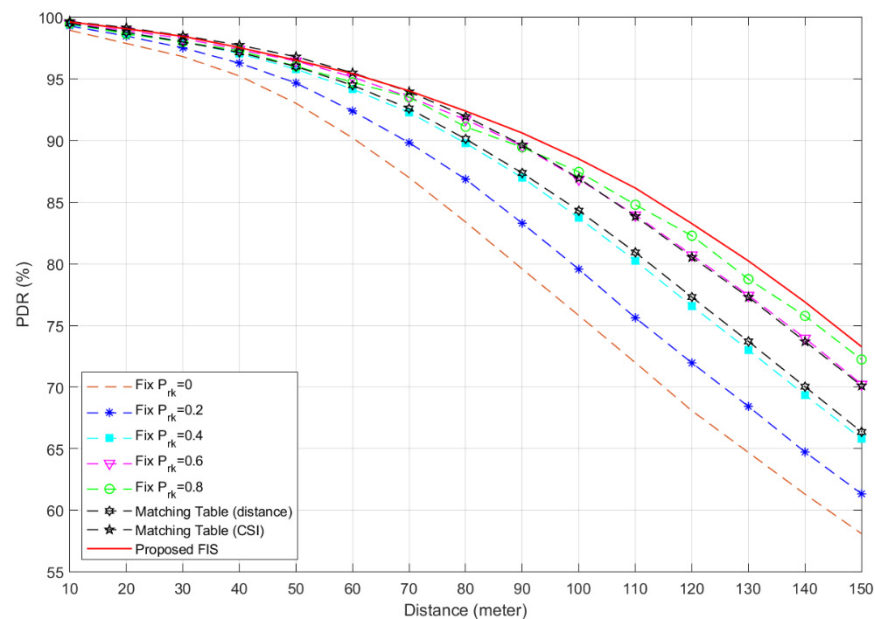


Figure 10. Overall PDR performance comparison for $n_V = 400$ vehicle scenario.

From the figures, it can be seen that the results from the proposed FIS method achieved the best overall PDR performance. In Figure 9, the performance improvement is slight. This occurred because the number of radio resources was adequate to serve the total number of vehicles, which was 200. Figure 9 shows that even though the performance difference was small, the proposed FIS proved it can contribute more to better performance results. For the results of the more congested scenario, as shown in Figure 10, it can be seen that the proposed FIS method underperformed for shorter vehicle distances. This result was achieved because, at shorter distances, many disturbances occur from the congested situation. Hence, some vehicles also suffer from a poor Line of Sight, significantly reducing the overall packet delivery performance. However, beyond the 70 m distances, the proposed FIS method outperformed the fixed P_{rk} value and the matching table methods.

It is possible that these results are limited to the performance results of a transmission power of 23 dBm. With the current transmission power, the vehicle communication coverage is affected. The increase in neighboring vehicle numbers also intensifies the competition for radio resources. The current simulation also used MCS 7 for all scenarios. Nevertheless, the role of P_{rk} in supporting the semipersistent foundation was well demonstrated. However, more research on this topic needs to be undertaken before the association between P_{rk} and PDR is more clearly understood.

The proposed FIS method proved that it can achieve better Packet Delivery Ratio (PDR) performance than the fixed Resource Keep Probability (P_{rk}) value and the matching table (if-condition) method. It can be seen from Figures 9 and 10 that the proposed FIS method outperformed the other methods in both sparse and crowded vehicle scenarios. Because the nature of the FIS relies on the fuzzy rule design, there is still much room for further enhancement.

5. Conclusions

The 3GPP C-V2X Mode 4 communication mode operates without Road-Side Unit (RSU) involvement. Hence, resource management is autonomously handled by the vehicle. A new resource management algorithm, called SB-SPS, was applied to accomplish the task. SB-SPS uses a probabilistic approach to ensure all vehicles serve the correct resource for data transmission. The Resource Keep Probability (P_{rk}) value is then used flexibly to govern the radio resources. With the corresponding P_{rk} value, the vehicle has a chance either to maintain its current radio resource slot or find a new one. The simulation results showed that by using the fixed P_{rk} value, the PDR performance still needs to be improved.

We designed a matching table simulation to explore the optimal adaptive solution for determining the P_{rk} value. Nevertheless, the matching table performed poorly. Hence, we proposed the FIS method with two inputs, distance and CSI, to derive fuzzy output P_{rk} . The simulation results showed that the proposed FIS method could outperform the other methods for either sparse or congested road conditions, with a total number of vehicles (n_V) of 200 and 400, respectively.

Author Contributions: Conceptualization, Y.-F.H. and J.-K.C.; Investigation, T.I.B. and Y.-F.H.; Methodology, T.I.B. and Y.-F.H.; Software, T.I.B. and J.-K.C.; Supervision, Y.-F.H. and J.-K.C.; Writing—Original Draft, T.I.B. and Y.-F.H.; Writing—Review and Editing, T.I.B. and Y.-F.H. All authors have read and agreed to the published version of the manuscript.

Funding: This work was supported by the Ministry of Science and Technology of Taiwan under grant MOST-111-2221-E-324-018.

Data Availability Statement: Not applicable.

Conflicts of Interest: The authors declare no conflict of interest.

References

- Zugno, T.; Drago, M.; Giordani, M.; Polese, M.; Zorzi, M. Toward Standardization of Millimeter-Wave Vehicle-to-Vehicle Networks: Open Challenges and Performance Evaluation. *IEEE Commun. Mag.* **2020**, *58*, 79–85. [CrossRef]
- TS 22.185; Technical Specification Group Services and System Aspects Service Requirements for V2X Services. Release 16. 3GPP, 2020. Available online: <https://portal.3gpp.org/desktopmodules/Specifications/SpecificationDetails.aspx?specificationId=2989> (accessed on 1 October 2022).
- Skouras, T.A.; Gkonis, P.K.; Ilias, C.N.; Trakadas, P.T.; Tsampasis, E.G.; Zahariadis, T.V. Electrical Vehicles: Current State of the Art, Future Challenges, and Perspectives. *Clean Technol.* **2020**, *2*, 1–16. [CrossRef]
- Gonzalez-Martin, M.; Sepulcre, M.; Molina-Masegosa, R.; Gozalvez, J. Analytical Models of the Performance of C-V2X Mode 4 Vehicular Communications. *IEEE Trans. Veh. Technol.* **2019**, *68*, 1155–1166. [CrossRef]
- Zhang, F.; Shan, L.; Zhao, X. Mathematical Representation for Reliability of Sensing-Based Semi-Persistent Scheduling in LTE-V2X. *IEEE Trans. Veh. Technol.* **2022**, *71*, 10115–10119. [CrossRef]
- Bazzi, A.; Cecchini, G.; Zanella, A.; Masini, B.M. Study of the Impact of PHY and MAC Parameters in 3GPP C-V2V Mode 4. *IEEE Access* **2018**, *6*, 71685–71698. [CrossRef]
- Bazzi, A.; Campolo, C.; Molinaro, A.; Berthet, A.O.; Masini, B.M.; Zanella, A. On Wireless Blind Spots in the C-V2X Sidelink. *IEEE Trans. Veh. Technol.* **2020**, *69*, 9239–9243. [CrossRef]
- Nkenyereye, L.; Nkenyereye, L.; Islam, S.M.R.; Kerrache, C.A.; Abdullah-Al-Wadud, M.; Alamri, A. Software Defined Network-Based Multi-Access Edge Framework for Vehicular Networks. *IEEE Access* **2020**, *8*, 4220–4234. [CrossRef]
- Choi, J.Y.; Jo, H.S.; Mun, C.; Yook, J.G. Deep Reinforcement Learning-Based Distributed Congestion Control in Cellular V2X Networks. *IEEE Wirel. Commun. Lett.* **2021**, *10*, 2582–2586. [CrossRef]
- Shan, L.; Wang, M.M.; Zhang, F.; Chen, S.; Zhang, J. Resource allocation for cellular device-to-device-aided vehicle-to-everything networks with partial channel state information. *Trans. Emerg. Telecommun. Technol.* **2022**, *33*, e4501. [CrossRef]
- Sabeeh, S.; Wesolowski, K.; Sroka, P. C-V2X Centralized Resource Allocation with Spectrum Re-Partitioning in Highway Scenario. *Electronics* **2022**, *11*, 279. [CrossRef]
- Sehla, K.; Nguyen, T.M.T.; Pujolle, G.; Velloso, P.B. Resource Allocation Modes in C-V2X: From LTE-V2X to 5G-V2X. *IEEE Internet Things J.* **2022**, *9*, 8291–8314. [CrossRef]
- Yoon, Y.; Kim, H. Resolving persistent packet collisions through broadcast feedback in cellular V2X communication. *Future Internet* **2021**, *13*, 211. [CrossRef]
- Yoon, Y.; Kim, H. An Evasive Scheduling Enhancement Against Packet Dropping Attacks in C-V2X Communication. *IEEE Commun. Lett.* **2021**, *25*, 392–396. [CrossRef]
- Skondras, E.; Michalakis, A.; Vergados, D.J.; Michailidis, E.T.; Miridakis, N.I.; Vergados, D.D. Network slicing on 5G vehicular cloud computing systems. *Electronics* **2021**, *10*, 1474. [CrossRef]
- Alghamdi, S.A. Novel path similarity aware clustering and safety message dissemination via mobile gateway selection in cellular 5G-based V2X and D2D communication for urban environment. *Ad Hoc Netw.* **2020**, *103*, 102150. [CrossRef]
- Kang, B.; Yang, J.; Paek, J.; Bahk, S. ATOMIC: Adaptive Transmission Power and Message Interval Control for C-V2X Mode 4. *IEEE Access* **2021**, *9*, 12309–12321. [CrossRef]
- Wu, T.; Yin, X.; Lee, J. A Novel Power Spectrum-Based Sequential Tracker for Time-Variant Radio Propagation Channel. *IEEE Access* **2020**, *8*, 151267–151278. [CrossRef]
- Bartoletti, S.; Masini, B.M.; Martinez, V.; Sarris, I.; Bazzi, A. Impact of the Generation Interval on the Performance of Sidelink C-V2X Autonomous Mode. *IEEE Access* **2021**, *9*, 35121–35135. [CrossRef]

20. Bayu, T.I.; Huang, Y.F.; Chen, J.K. Performance of C-V2X Communications for High Density Traffic Highway Scenarios. In Proceedings of the 2021 International Conference on Technologies and Applications of Artificial Intelligence, Taichung, Taiwan, 18 November 2021; pp. 228–233.
21. Fan, C.; Li, B.; Wu, Y.; Zhang, J.; Yang, Z.; Zhao, C. Fuzzy Matching Learning for Dynamic Resource Allocation in Cellular V2X Network. *IEEE Trans. Veh. Technol.* **2021**, *70*, 3479–3492. [[CrossRef](#)]
22. Alghamdi, S.A. Emperor based resource allocation for D2D communication and QoF based routing over cellular V2X in urban environment (ERA-D2Q). *Wirel. Netw.* **2020**, *26*, 3419–3437. [[CrossRef](#)]
23. Zhang, M.; Dou, Y.; Chong, P.H.J.; Chan, H.C.B.; Seet, B.C. Fuzzy Logic-Based Resource Allocation Algorithm for V2X Communications in 5G Cellular Networks. *IEEE J. Sel. Areas Commun.* **2021**, *39*, 2501–2513. [[CrossRef](#)]
24. Bazzi, A.; Cecchini, G.; Menarini, M.; Masini, B.M.; Zanella, A. Survey and perspectives of vehicular Wi-Fi versus sidelink cellular-V2X in the 5G era. *Future Internet* **2019**, *11*, 122. [[CrossRef](#)]
25. Yin, J.; Hwang, S.H. Adaptive sensing-based semipersistent scheduling with channel-state-information-aided reselection probability for LTE-V2V. *ICT Express* **2022**, *8*, 296–301. [[CrossRef](#)]
26. Huang, Y.F.; Bayu, T.I.; Liu, S.H.; Huang, H.Y.; Huang, W. Applications of Fuzzy Inference System on V2V Routing in Vehicular Networks. In *Intelligent Information and Database Systems; Lecture Notes in Computer; Springer: Cham, Switzerland, 2020; pp. 255–265.*
27. *TS 36.101*; Technical Specification Group Radio Access Network Evolved Universal Terrestrial Radio Access (E-UTRA) User Equipment (UE) Radio Transmission and Reception. Release 14. 3GPP, 2017. Available online: <https://portal.3gpp.org/desktopmodules/Specifications/SpecificationDetails.aspx?specificationId=2411> (accessed on 1 October 2022).
28. *TS 36.213*; Technical Specification Group Radio Access Network Evolved Universal Terrestrial Radio Access (E-UTRA) Physical Layer Procedures. Release 14. 3GPP, 2017. Available online: <https://portal.3gpp.org/desktopmodules/Specifications/SpecificationDetails.aspx?specificationId=2427> (accessed on 1 October 2022).
29. *TS 36.321*; Technical Specification Group Radio Access Network Evolved Universal Terrestrial Radio Access (E-UTRA) Medium Access Control (MAC) Protocol Specification. Release 14. 3GPP, 2017. Available online: <https://portal.3gpp.org/desktopmodules/Specifications/SpecificationDetails.aspx?specificationId=2437> (accessed on 1 October 2022).
30. Huang, Y.F. Performance of Adaptive Multistage Fuzzy-Based Partial Parallel Interference Canceller for Multi-Carrier CDMA Systems. *IEICE Trans. Commun.* **2005**, *E88-B*, 134–140. [[CrossRef](#)]
31. Cecchini, G.; Bazzi, A.; Masini, B.M.; Zanella, A. LTEV2Vsim: An LTE-V2V simulator for the investigation of resource allocation for cooperative awareness. In Proceedings of the 2017 5th IEEE International Conference on Models and Technologies for Intelligent Transportation Systems (MT-ITS), Naples, Italy, 26–28 June 2017; pp. 80–85.